TWENTYFIFTH EUROPEAN ROTORCRAFT FORUM

Paper No: H3

FLIGHT ENVELOPE LIMIT DETECTION AND AVOIDANCE

BY

JOE HORN, ANTHONY J. CALISE, J.V.R. PRASAD
GEORGIA INSTITUTE OF TECHNOLOGY
USA

SEPTEMBER 14-16,1999
ROME
ITALY

ASSOCIAZIONE INDUSTRIE PER L'AEROSPAZIO,I SISTEMI E LA DIFESA
ASSOCIAZIONE ITALIANA DI AERONAUTICA ED ASTRONAUTICA

Flight Envelope Limit Detection and Avoidance for Rotorcraft

Joe Horn, Graduate Student

Anthony J. Calise, Professor

J.V.R. Prasad, Professor

School of Aerospace Engineering
Georgia Institute of Technology
Atlanta, GA

Abstract

Modern rotorcraft are constrained by complex flight envelopes. Simplified operational envelopes restrict the true maneuvering performance of the aircraft. Tactile cueing systems can be used to protect against envelope violations and provide carefree handling qualities, but require algorithms to detect approaching limits before they are exceeded. Dynamic trim estimation using neural networks is an effective method for detecting limits that are reached in quasi-steady flight. The method is extended to include adaptation to variations in weight and balance parameters or modeling errors. The system is applied to provide angle of attack and load factor protection on the XV-15. A pilot model is developed to demonstrate the effectiveness of the limit avoidance system. The system has also been tested in real-time piloted simulation. A modified algorithm is developed to provide envelope cueing for parameters that impinge on limits in the transient response and is applied to limit longitudinal flapping on the XV-15.

Nomenclature

Mathematical Symbols:

A_p, A_t	=	Pilot Aggressiveness Factors
A,B,C	=	State-Space Dynamics Matrices
B_1	=	Longitudinal Cyclic
f, g, h	=	Vector Functions
e	=	Error Vector
F	=	Stick Force
g	=	Acceleration of Gravity
G	=	Linear Transfer Function
h	=	Altitude
N_z	=	Normal Load Factor
q	=	Pitch Rate
Q	=	Torque
s	=	Laplace Operator
u	=	Longitudinal Body-Axis Velocity
w	=	Vertical Body-Axis Velocity
u	=	Control Vector
V	=	Airspeed
W	=	NN Weights
x	=	State Vector
y	=	Limited Parameter Vector
α	=	Angle of Attack
β_{long}	=	Long. Flapping Angle
β	=	ANN Basis Functions
δ	=	Control Deflection
δ_e	=	Elevator Actuator Position
γ	=	Glide Path Angle
θ	=	Pitch Attitude

Subscripts:

coll	=	Collective
DT	=	Dynamic Trim
e	=	Equilibrium
f, fast	=	Fast Dynamics
H	=	High Limit
I	=	Instantaneous
L	=	Low Limit
lat	=	Lateral
lim	=	Limit
long	=	Longitudinal
p	=	Predicted
pk	=	Peak
s, slow	=	Slow Dynamics

Acronyms:

AFCS	=	Automatic Flight Control System
ANN	=	Adaptive Neural Network
AOA	=	Angle of Attack
FBW	=	Fly-by-wire
NN	=	Neural Network
SCAS	=	Stability and Command Augmentation System

1. Introduction

Recently there has been increased emphasis on the need for carefree handling capability on military rotorcraft. Rotorcraft tend to have complex envelopes that define the performance and maneuvering capability of the aircraft. The boundaries of the flight envelopes include structural and controllability constraints associated with the V-n envelope and torque limits, as well as more complicated mechanical constraints such as flapping limits. Because of the complexity and pilot workload requirements associated with the true flight envelope, simplified operational envelope limits are often used. The simplified envelopes are conservative and tend to restrict the true performance of the aircraft while still requiring significant pilot workload to monitor the limits. The ability to safely fly to the edges of the true operational envelope of the aircraft within reasonable pilot workload constraints would be a highly desirable feature for future military helicopters. Envelope protection systems have the capability to increase the usable agility of the aircraft while improving handling qualities and flight safety.

A flight envelope limiting or carefree handling control system must perform two functions – limit detection and limit avoidance. The system must detect the encroachment of an envelope limit, and then it must take measures to prevent the violation of the limit. One approach is to use direct sensor measurement to detect the limit, and then intervene directly via a fly-by-wire (FBW) control system to ensure limit avoidance. This is typically done by phasing in a command following control law that prevents limit violations in the extreme ranges of control travel. This approach has been applied to fixed-wing aircraft for load factor and stall protection [1, 2], and to rotorcraft for torque and rotor speed protection [3, 4, 5]. Similar techniques have been applied for structural load limiting (SLL) control laws on the V-22 [6, 7]. This approach has been shown to effectively prevent envelope violations in a way that is transparent to the pilot. However, for some applications, the use of feedback control to provide envelope limiting has certain limitations:

- The necessary sensor data is not always available.
- The limiting feedback can change the response characteristics of the aircraft and thereby confuse the pilot or degrade handling qualities.
- There is no inherent override capability if the pilot needs to violate a limit in an emergency situation.
- The pilot may not be aware of approaching limits.
- Many rotorcraft are not equipped with full authority FBW control systems.

The direct feedback approach tends to further disassociate the pilot from the envelope limits. In fact, the use of full-authority FBW control systems introduces new envelope limit problems in the form of control saturation limits.

An alternative approach to limit avoidance is to provide some form of enhanced cueing to the pilot. Simulation studies have shown that tactile feedback in the pilot control inceptors is the most effective means of envelope limit cueing [8, 9]. The tactile cueing can take the form of a "soft stop" in the force feel curve of the control stick.

When using a pilot cueing system it is desirable that the limit detection algorithm estimate *future* values of a limited parameter in order to provide a sufficient time margin for the pilot to react to the cue. Certain combinations of large control inputs might create a situation where a limit violation is unavoidable. Because there is a time lag between the pilot control input and the aircraft response, a limit avoidance cueing system based on *instantaneous* data would allow such inputs and therefore would not be a reliable envelope protection system. Thus, it is necessary to achieve a prediction lead time. This paper discusses limit detection algorithms which predict future values of a limited parameter given the pilot control inputs, and inversely, calculate estimates of the control deflections which will cause the parameter to reach a specified envelope limit at some future time. These data are used to drive a variable force-feel system to cue the pilot of the approaching limit *before* it is exceeded.

Studies have shown the capability of neural networks to synthesize complex loads data by training the network with flight test data from an instrumented aircraft [10, 11]. In these studies, the neural networks were trained to generate instantaneous data. It was shown in ref. 9, that a prediction lead time can be obtained by training the neural network to model future values of a parameter by using a time shift in the input and output training data. The selection of the time shift is not trivial, and the optimal value may vary with flight condition or type of limit.

The dynamic trim estimation algorithm achieves a prediction lead time by estimating the quasi-steady-state (or dynamic trim) value of a limited parameter. A neural network is used to model the mapping between the pilot controls and the aircraft limits in dynamic trim. This approach was used to provide angle of attack and load factor limit cueing through the longitudinal stick on the V-22 aircraft [12]. The system was demonstrated in piloted simulation and shown to substantially improve both usable agility and flight safety. A similar system was applied to provide V-n envelope limiting on the XV-15 aircraft and was demonstrated in batch simulations [13].

A restriction on the dynamic trim estimation approach to envelope protection is that it requires accurate models of the dynamic trim characteristics over all possible flight conditions. The method has recently been extended to incorporate an adaptive scheme which uses sensor data to correct the prediction algorithm [14]. Another restriction is that the dynamic trim method is not effective for parameters such as rotor flapping, which tends to overshoot their steady-state value, and exceed limits in the transient response. An algorithm was developed to estimate the peak response characteristics of a limited parameter and applied to limit longitudinal flapping angle [14]. This paper reviews recent developments in the dynamic trim estimation and peak response estimation algorithms and new results are shown using a simulated pilot model.

2. Envelope Limiting Using Dynamic Trim Estimation

Dynamic trim is a quasi-steady maneuvering flight condition, in which the fast aircraft states (e.g. angular rates) have reached steady-state while the slow states (e.g. airspeed, Euler angles) may be varying in time. For example, in a transient turn, angular accelerations will occur primarily at the initiation of the maneuver. As the pilot sustains the maneuver the aircraft will hold constant angular rates, while slow states such as airspeed might vary throughout the entire maneuver. The pilot and AFCS tend to regulate the aircraft about a dynamic trim equilibrium. V-n envelope parameters such as load factor and angle-of-attack tend to approach the envelope limits as the aircraft reaches dynamic trim.

A systematic approach for envelope limiting based on dynamic trim has been developed in previous work [12, 13]. The aircraft states are partitioned into fast and slow dynamics. Considering the longitudinal dynamics of the XV-15 in airplane mode, AOA and pitch rate are treated as fast states (short period mode), while airspeed, altitude, and rate of climb are treated as slow states (phugoid mode):

$$\begin{gathered}\dot{\mathbf{x}} = \mathbf{g}(\mathbf{x},\mathbf{u}),\ \mathbf{x} = \left[\mathbf{x}_{\text{slow}}^{\text{T}} \quad \mathbf{x}_{\text{fast}}^{\text{T}}\right]^{\text{T}} \\ \mathbf{x}_{\text{slow}} = \left[V \quad \gamma \quad h\right]^{\text{T}},\ \mathbf{x}_{\text{fast}} = \left[q \quad \alpha\right]^{\text{T}} \\ \mathbf{u} = \left[\delta_{long} \quad \delta_{coll}\right]^{\text{T}} \\ \mathbf{y} = \left[Q \quad \alpha \quad N_z \quad \dot{V}\right]^{\text{T}} = \mathbf{h}(\mathbf{x},\mathbf{u})\end{gathered} \tag{1}$$

In dynamic trim, the fast states reach equilibrium, and the limited parameters in dynamic trim can be shown to be a function of the pilot controls and the slow states:

$$\mathbf{y}_{\text{p}} = \mathbf{f}(\mathbf{x}_{\text{s}},\mathbf{u}) = \mathbf{f}(V,\gamma,h,\delta_{long},\delta_{coll}) \tag{2}$$

The function on the right hand side of eqn. 2, is a highly non-linear function of five variables (and becomes a function of even more variables when including lateral degrees of motion). Neural networks are an efficient means for modeling complex non-linear functions of many variables. A function of several variables, which could be modeled by a large multi-dimensional table look-up, can be accurately and more efficiently represented by a neural network that is trained using a relatively small number of randomly scattered data points A non-linear simulation model [15] was used to generate training data and to evaluate the systems. A modified trim algorithm was used to generate multiple dynamic trim points for training.

The predictive capability of dynamic trim estimation is illustrated in Figure 1, which shows a typical transient response of the neural network as compared to the simulated response of the XV-15 for an aft longitudinal step input. The neural network responds immediately to the pilot control input and then converges with the aircraft response as it approaches dynamic trim. The limit avoidance systems has a couple of seconds of lead time to cue the pilot.

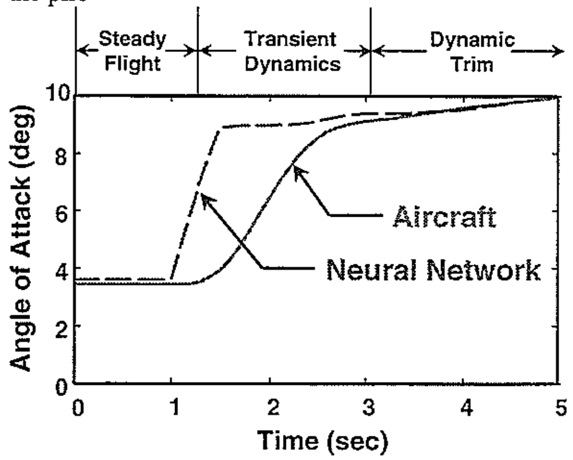

Figure 1 Dynamic Trim Limit Prediction

An approximate pseudo-inversion of the functions in **f** is used to determine the smallest combination of control inputs that will cause the envelope limit to be violated – the critical control margin vector.

$$\Delta\mathbf{u}_i^* = \left(\frac{\partial f_i}{\partial \mathbf{u}}\right)^+ \left(y_{\text{lim}} - y_p - \frac{\partial \mathbf{f}}{\partial \mathbf{x}_s}\dot{\mathbf{x}}_s \Delta t\right) \tag{3}$$

The logical approach to envelope cueing is to increase the force resistance on the stick as the control margin to the limit becomes small. The control margin is calculated as a vector, so the increase in force can occur in multiple axes in a manner that optimally reduces the chance of an envelope violation. If only one control axis is considered, equation 6 effectively defines a "soft stop" location in the control travel.

2. 1 Real-Time Piloted Simulation Results

An envelope cueing system based on dynamic trim was developed to provide angle-of-attack and load factor limiting on the V-22 [12] and demonstrated in piloted simulation. The angle-of-attack limit is associated with a buffet that occurs at high mach numbers and is the primary restriction on the maneuvering ability of the aircraft at high speeds. The envelope cueing system was evaluated in piloted simulation for a high speed wind up turn maneuver. The pilot descends as rapidly as possible starting at an altitude of about 15000 ft towards a location on the ground. In order to maintain a desired airspeed and to stay over a ground location the pilot makes a high-g banked turn throughout the maneuver. During such a maneuver, the angle-of-attack limit restricts the maneuvering capability of the aircraft and therefore restricts the maximum safe rate of descent. The angle-of-attack limit varies throughout the maneuver due to variation in the mach number with altitude and it is difficult for the pilot to fly along the boundary of the AOA / Mach envelope without special cueing. The envelope cueing provided a soft stop in the longitudinal control axes as the aircraft approached the limit. Figure 2 shows sample flight trajectories relative to the envelope with and without the envelope cueing. The results show that the pilot could safely fly closer to the edge of the envelope with the cueing. The experiment was repeated with three different pilots, and Figure 3 shows the overall results – an effective increase in both usable agility and safety. Because the pilots could safely fly at a higher g level, they could descend more rapidly and therefore reduce the task time.

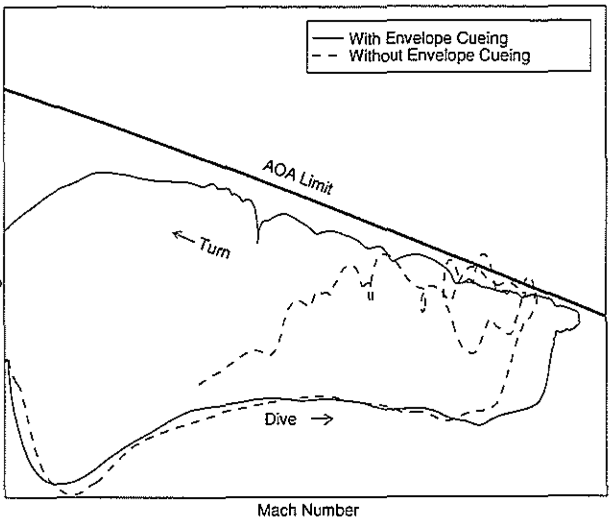

Figure 2 Sample Trajectories in AOA / Mach Envelope

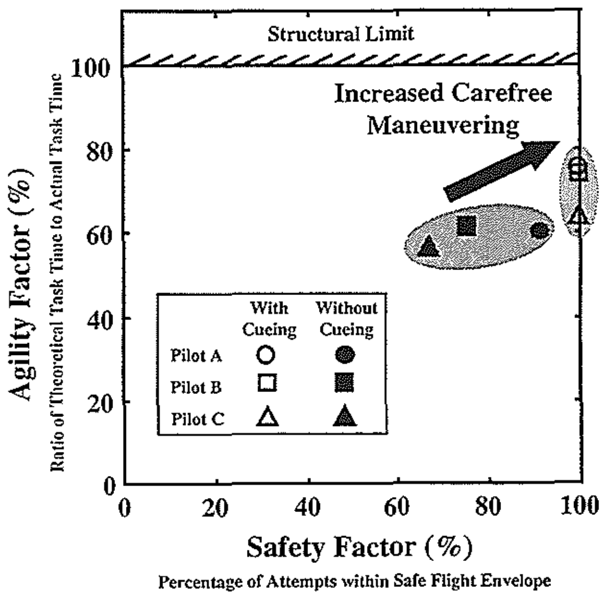

Figure 3 Increased Carefree Maneuvering

2. 2 Simulation Using a Pilot Model

In order to study the envelope protection system in conditions with multiple limits, a mathematical representation of a pilot was used to "fly" the aircraft through a series of aggressive maneuvers. The pilot was modeled as a simple outer loop guidance law using energy feedback to control the flight path angle and airspeed. The guidance laws in the pitch and thrust axes were scaled by aggressiveness factor $[A_p, A_t]$ in order to test the system over a range of pilot gains. The pilot model provides control forces on the collective and longitudinal levers and interaction of the pilot and the force-feel systems is represented by a simple spring-mass-damper system. The envelope protection cues are modeled as a force increment that counters the pilot's applied force. This approach was used to study a V-n envelope and torque limiting system on the XV-15. The pilot model simulation is illustrated in Figure 4.

The load factor envelope was set between +2.5 g and -1.0 g, the AOA limits at +15 deg and -10 deg, and the torque envelope between 0% and 100%. An aggressive push-over followed by a pull-up maneuver was simulated by ramping in –30° and +30° flight path commands, and the airspeed command is set to hold the initial speed of 153 knots. The magnitude of the commands are intentionally set so that it is impossible for the aircraft to track the commands within the envelope constraints of the aircraft.

Figures 5 and 6 show the time history of the limited parameters with and without envelope protection. For the given aggressiveness level (A_p=3, A_t=1), Figure 5 shows that the load factor, AOA, and torque envelopes are violated severely without envelope protection. Figure 6 shows that envelope limiting force-feel feedback effectively allows the pilot model to fly the aircraft along the boundaries of the envelope without exceeding limits. The results are consistent with the piloted simulation study of the V-22, but in this case the system effectively protects against multiple limits (load factor, angle-of-attack, and torque) simultaneously and the force-feel cues are applied in multiple control axes (collective and longitudinal stick). Figure 7 shows similar results in which the pilot model commands a symmetric pull-up / push-over maneuver and allows airspeed to vary. The envelope trajectories show that the envelope limiting is effective in the AOA / load factor corner of the envelope.

3. Adaptive Dynamic Trim Estimation

The dynamic trim estimation algorithm has the benefit that direct measurement of the limited parameter is not required. However, it is necessary that a sufficient quantity of training data be generated to accurately model the dynamic trim characteristics over all possible operating conditions. In some applications, sensors may be available to give reliable data on the instantaneous value of a limited parameter, but dynamic trim estimation is still desirable in order to have a prediction lead time. One can use sensor data to supplement the dynamic trim estimation algorithm by correcting inaccuracies in the algorithm due to modeling errors and unmodeled configuration changes. For example, the weight and balance properties of the aircraft will vary significantly during normal operation. Training the network over all weight and balance configurations would require additional network inputs and a geometric increase in the amount of training data required. Alternatively, the neural network might be trained at one particular weight and center of gravity location, and an adaptive scheme can be used to correct the errors in the network response based on sensor data. This represents a trade-off between the relative cost of additional sensors to that of generating larger training data sets and larger networks. In the case of load factor and AOA limiting, it is likely that the required sensor data is already available to implement an adaptive dynamic trim estimation scheme.

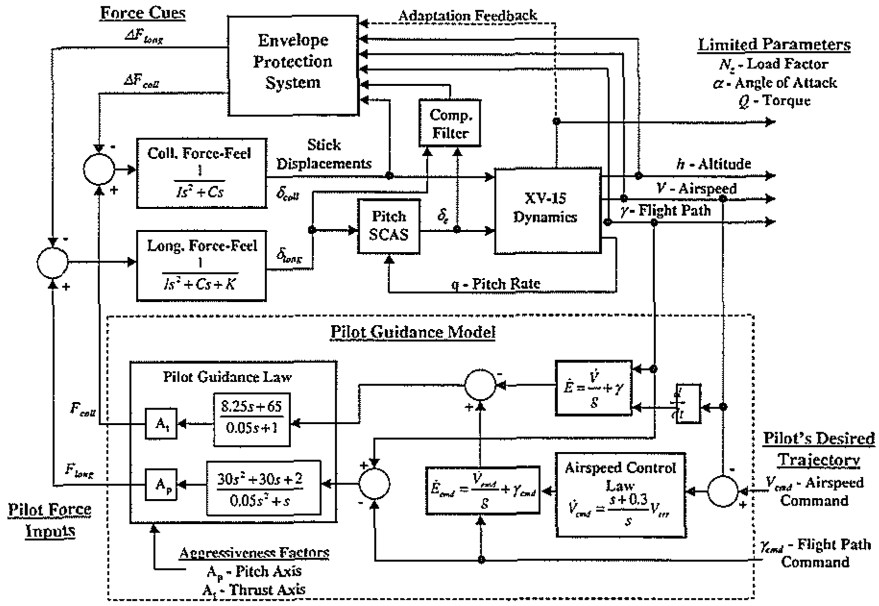

Figure 4 Pilot Model Simulation of Envelope Limiting System

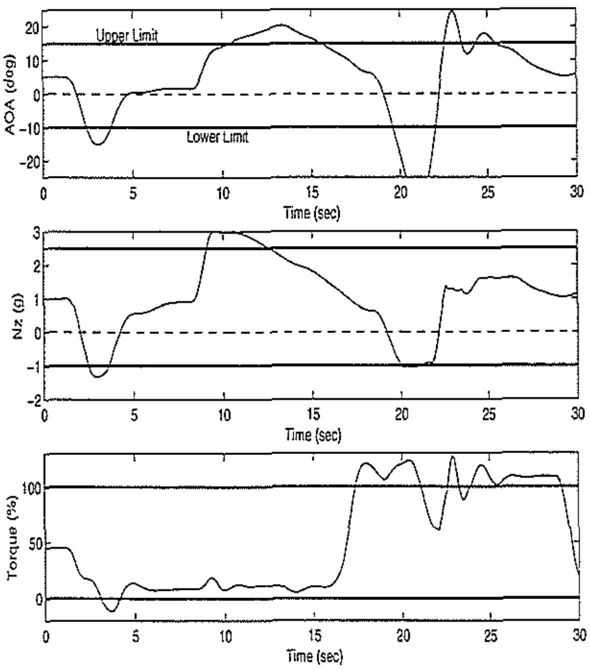

Figure 5 Results without Envelope Protection

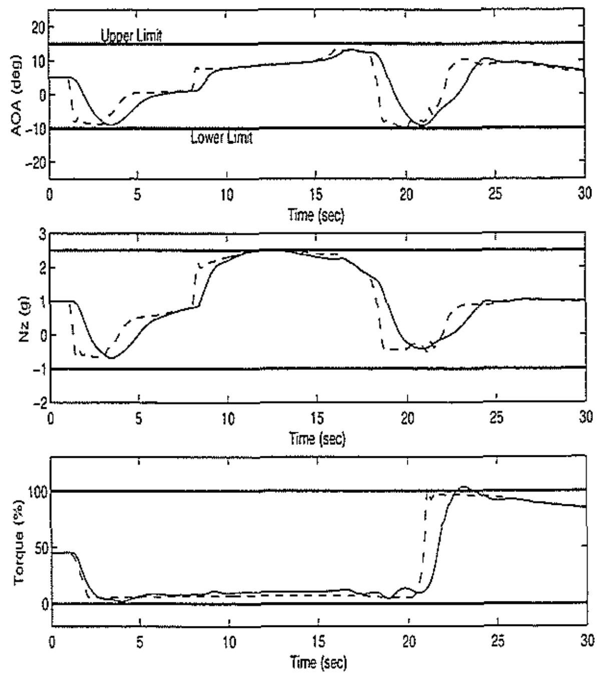

Figure 6 Results with Envelope Protection

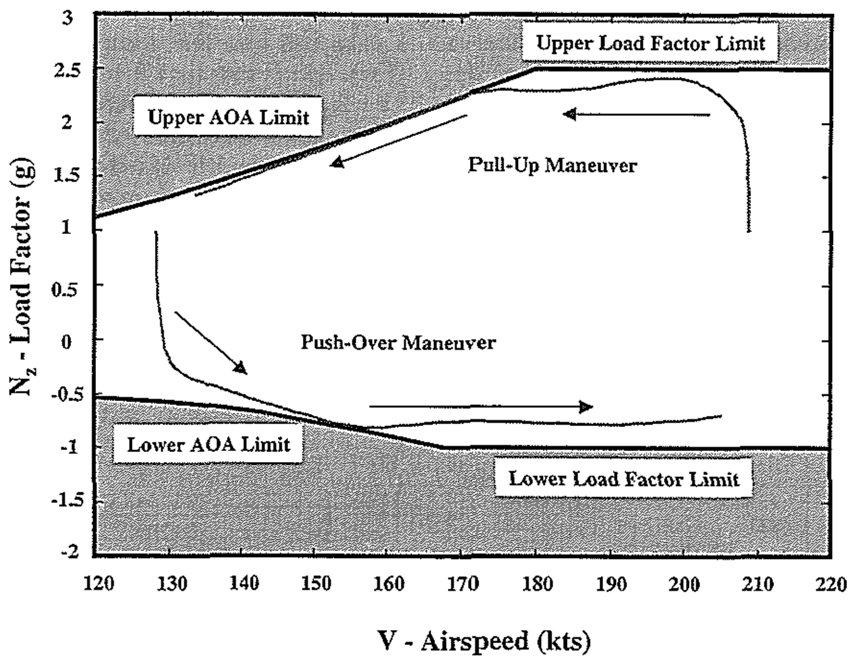

Figure 7 Pull-Up / Push-Over Maneuvers with V-n Envelope Protection

An adaptive single layer sigma-pi network, similar to that recently developed for adaptive control of tilt-rotor aircraft [16], is used to make an additive correction to the output from the existing static network. The ANN learns to model the error between the static network and the actual dynamic trim response of the aircraft. The main difficulty lies in the need to generate an appropriate error signal to drive the ANN update law. The sensor data represents the instantaneous response, while the output of the network represents the estimated dynamic trim response. The solution is to use a filtering scheme to generate comparable signals. The architecture of the adaptive estimation scheme is illustrated in Figure 8.

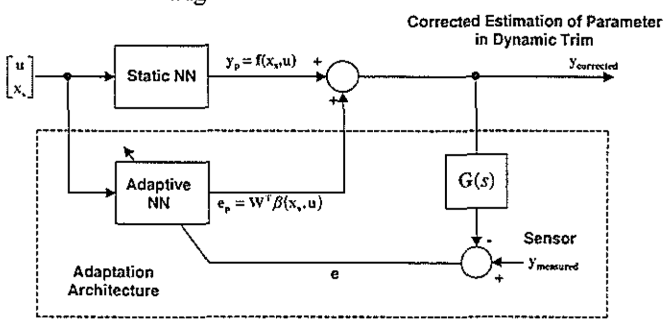

Figure 8 Adaptive Dynamic Trim Estimation

The filter G(s) is selected to approximate the dynamic characteristics of the limited parameter. Since, the dynamic trim response represents an equilibrium condition, the instantaneous response can be approximated by a linear filter with a unity steady-state gain driven by the dynamic trim value. In the case of load factor and AOA, a low-pass second order filter suffices:

$$\mathbf{y}_{\mathrm{I}} \approx \mathbf{G}(s)\mathbf{y}_{\mathrm{DT}}$$

$$\mathbf{G}(s) = \begin{bmatrix} \left(\dfrac{\omega_n^2}{s^2 + 2\xi\omega_n s + \omega_n^2}\right)_1 & & 0 \\ & \ddots & \\ 0 & & \left(\dfrac{\omega_n^2}{s^2 + 2\xi\omega_n s + \omega_n^2}\right)_k \end{bmatrix} \quad (4)$$

where the subscripts I and DT denote instantaneous and dynamic trim values respectively. Thus, the output of the filter in Figure 8, represents the instantaneous response of the limited parameters corresponding to the neural network's estimate of the dynamic trim response. This signal may be compared directly with the sensor measurement of the limited parameter to generate an error signal.

The output of the ANN is a polynomial of the network inputs (the slow states and control inputs), where the coefficients of the polynomial are the network weights. In this example we consider AOA and load factor limits on the XV-15 in longitudinal flight. The ANN can be represented mathematically:

$$\begin{gathered} \mathbf{y}_{\mathrm{p}} = [\alpha \quad N_z]^T, \mathbf{x}_s = [V \quad \gamma \quad h]^T, \mathbf{u} = [\delta_{long} \quad \delta_{col}]^T \\ \mathbf{e}_{\mathrm{p}} = \mathbf{W}^{\mathrm{T}}\boldsymbol{\beta}(\mathbf{x}_s, \mathbf{u}) \\ \mathbf{C}_1 = [1 \quad V \quad V^2 \quad \gamma]^T \\ \mathbf{C}_2 = [1 \quad \delta_{long} \quad \delta_{long}^2 \quad \delta_{long}^3 \quad \delta_{coll}]^T \\ \boldsymbol{\beta}(\mathbf{x}_s, \mathbf{u}) = \mathbf{C}_1 \otimes \mathbf{C}_2 \text{ where } \otimes \text{ is Kronecker product} \\ \Rightarrow \mathbf{e}_{\mathrm{p}} = \mathbf{W}_1 + \mathbf{W}_2\delta_{long} + \mathbf{W}_2\delta_{long}^2 + \cdots + \mathbf{W}_i V\delta_{long} + \cdots \end{gathered} \quad (5)$$

The network basis functions, β, are just powers and cross products of the input data. In practice, the input data is scaled to avoid large variations in scale between the different weights.

The appropriate update law can be derived from Lyapunov theory. Using the following assumptions:

- The dynamics of G(s) are stable.
- The filter, G(s), is an accurate model of the dynamics of the limited parameter.
- There exist a set of ideal weights that allow the ANN to exactly correct the error of the static network.

One arrives at the following error dynamics:

$$\ddot{e} + 2\zeta\omega_n\dot{e} + \omega_n^2 e = \tilde{W}^T\beta(x_s,u) \tag{6}$$

where the tilde denotes the difference between the network weights and the ideal weights. Using a similar technique as in ref. 16, Lyapunov analysis results in the following weight update law:

$$\dot{W} = \gamma\beta(x_s,u)(P_{12}e + P_{22}\dot{e})^T\omega_n^2 \tag{7}$$

where the P matrix solves the Lyapunov equation:

$$A = \begin{bmatrix} 0 & I \\ -\omega_n^2 & -2\zeta\omega_n \end{bmatrix}, P = \begin{bmatrix} P_{11} & P_{12} \\ P_{21} & P_{22} \end{bmatrix} \tag{8}$$
$$A^T P + PA = -I$$

In reality, a single-layer network cannot exactly model the error in the dynamic trim estimate. Despite this, more advanced analysis in ref. 16 shows that the error dynamics will at least be bounded.

The adaptive dynamic trim estimation scheme was evaluated using pilot model simulation of the XV-15 aircraft in longitudinal flight, similar to the results from the previous section. The adaptation is used to correct the estimates of AOA and load factor when the longitudinal CG location is shifted from the value used when training the static network. The pilot model was used to simulate the same push-over and pull-up maneuver as in Figures 5 and 6, but the CG is set five inches aft. Figure 9 shows that the performance of the envelope protection system is degraded with no adaptation. Although the estimated dynamic trim response is kept within the limits, the estimates are erroneous, which allows the actual response of the aircraft to violate the envelope limits.

The same maneuver was then simulated with the adaptation algorithm engaged. The maneuver was repeated three times to allow the ANN weight to adjust to the new C.G. location. Figure 10 shows the performance of the envelope limiting system after the ANN has had time to learn the dynamic trim estimation error. The results show that the corrected estimation is more accurate and the system is more effective in preventing envelope violations.

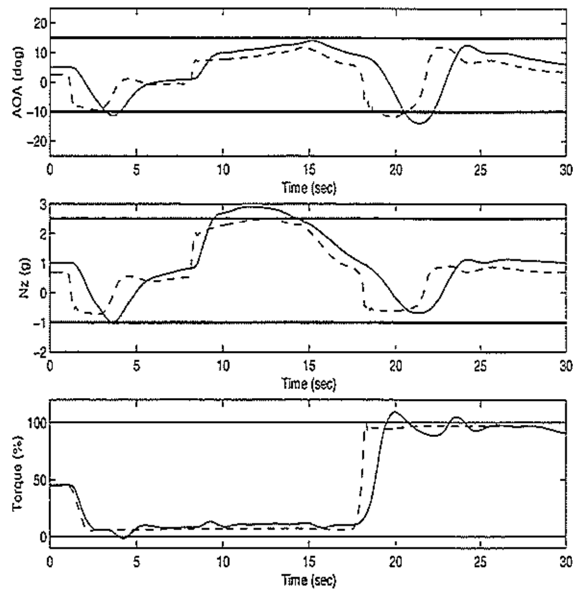

Figure 9 Results with Aft C.G., No Adaptation

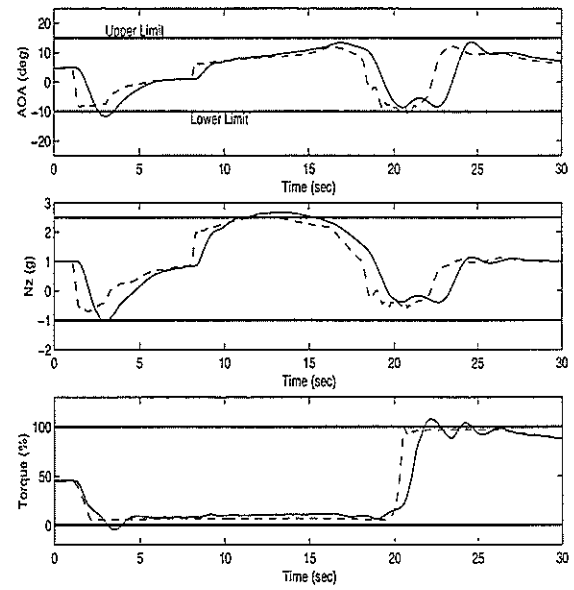

Figure 10 Results with Aft C.G., With Adaptation

4. Envelope Limiting Using Peak Response Estimation

The dynamic trim estimation approach is only applicable for limiting the steady state response of a limited parameter. In the case of flapping limits, the steady-state response is not critical. Instead, one must consider the peak transient response. The peak response can be estimated using an approximate linear model of the dynamics of the parameter about the dynamic trim equilibria. Consider the non-linear equations of motion for longitudinal flight of the XV-15 in helicopter mode. In this example, longitudinal flapping angle is to be limited within set mechanical limits.

$$\begin{gathered}
\dot{\mathbf{x}} = \mathbf{g}(\mathbf{x}_s, \mathbf{x}_f, \mathbf{u}) \\
\mathbf{x}_s = [u \quad w \quad \theta]^T, \quad \mathbf{u} = [\delta_{long} \quad \delta_{coll}]^T \\
\mathbf{x}_f = [q \quad B_1 \quad + \text{control system states} \quad \cdots]^T \\
\mathbf{y} = \beta_{long} = \mathbf{h}(\mathbf{x}_s, \mathbf{x}_f, \mathbf{u})
\end{gathered} \tag{9}$$

The function $\mathbf{h}$ returns the instantaneous value of the limited parameter given the controls and full state vector as input. In general, the limited parameters are unmeasured quantities and complex non-linear functions of the states. In this example, it is assumed that there is no flapping sensor. A multi-layer neural network is used to model the *instantaneous* response of flapping as function of the aircraft states (which are assumed to be measured). The network was trained using a collection of time history data generated by the XV-15 GTRSim model.

The linearized dynamics of the XV-15 are represented in Figure 11. This 10[th] order linear system includes actuator dynamics and the longitudinal SCAS.

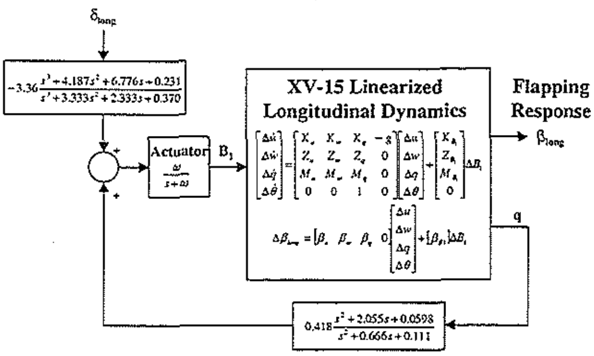

Figure 11 Linearized Longitudinal Dynamics of the XV-15 in Helicopter Mode

Calculating the peak response of such a system results in an intractable numerical problem. Thus, we seek a simplified 2[nd] order model that gives a reasonable approximation of the dynamics over the most critical operating frequencies. This can be achieved by removing the slow dynamics from the aircraft equations of motion, since the flapping peak response is expected to occur at much faster time scales, and then performing balanced model reduction to eliminate the additional states associated with the SCAS transfer functions. The resulting 2[nd] order model can be represented in state-space:

$$\begin{gathered}
\begin{bmatrix} \Delta\dot{q} \\ \Delta\dot{B}_1 \end{bmatrix} = \mathbf{A}\begin{bmatrix} \Delta q \\ \Delta B_1 \end{bmatrix} + \mathbf{b}\delta_{long} \\
\Delta\beta_{long} = \mathbf{C}\begin{bmatrix} \Delta q \\ \Delta B_1 \end{bmatrix} \\
\Delta q = q - q_e, \; \Delta B_1 = B_1 - B_{1_e}
\end{gathered} \tag{10}$$

The $\mathbf{C}$ matrix is calculated by perturbing the neural network that models the function $\mathbf{h}$, in order to determine the sensitivity of flapping to pitch rate and longitudinal cyclic.

$$\mathbf{C} = \begin{bmatrix} \dfrac{\partial \mathbf{h}}{\partial q} & \dfrac{\partial \mathbf{h}}{\partial B_1} \end{bmatrix} = \begin{bmatrix} \dfrac{\partial \beta_{long}}{\partial q} & \dfrac{\partial \beta_{long}}{\partial B_1} \end{bmatrix} \tag{11}$$

The $\mathbf{A}$ and $\mathbf{b}$ matrices and the equilibrium states are a function of the flight condition.

$$[q_e \quad B_{1_e} \quad \mathbf{A} \quad \mathbf{b}]^T = \mathbf{f}(\mathbf{x}_s, \mathbf{u}) \tag{12}$$

These parameters were calculated for the XV-15 at 20 knot intervals from 20 knots rearward flight to 120 knots forward flight and scheduled by airspeed into the envelope limiting system. The variations of these parameters for climbing and descending flight were neglected.

Given a second order state-space model, the response for a step input with arbitrary initial conditions can be calculated:

$$\begin{aligned}
\Delta\beta_{long}(t) = {} & \left[k_1\left(1 - \frac{e^{-\zeta\omega_n t}}{\sqrt{1-\zeta^2}}\sin(\omega_d t + \theta)\right) + k_2\frac{e^{-\zeta\omega_n t}}{\sqrt{1-\zeta^2}}\sin(\omega_d t)\right]\Delta\delta_{long} + \\
& \left[\frac{e^{-\zeta\omega_n t}}{\sqrt{1-\zeta^2}}\sin(\omega_d t)\mathbf{k}_3 + \left(e^{-\zeta\omega_n t}\cos(\omega_d t) - 1\right)\mathbf{k}_4\right]\begin{bmatrix} \Delta q \\ \Delta B_1 \end{bmatrix}
\end{aligned} \tag{13}$$

$$\text{where} \quad \omega_n = \sqrt{\det \mathbf{A}}, \quad \zeta = -\frac{\operatorname{tr}\mathbf{A}}{2\omega_n}, \quad \omega_d = \sqrt{1-\zeta^2}\,\omega_n, \quad \theta = \tan^{-1}\frac{\zeta}{\beta}$$

$$k_1 = \frac{\mathbf{C}\operatorname{adj}(-\mathbf{A})\mathbf{b}}{\omega_n^2}, \quad k_2 = \frac{\mathbf{C}\mathbf{b}}{\omega_n}, \quad \mathbf{k}_3 = \frac{\mathbf{C}\operatorname{adj}(-\mathbf{A}) - \xi\omega_n\mathbf{C}}{\omega_n}, \quad \mathbf{k}_4 = \mathbf{C}$$

Time to peak is given by:

$$t_{pk}(\Delta u, \Delta q, \Delta B_1) = \frac{1}{\omega_d}\tan^{-1}\left(\sqrt{1-\zeta^2}\,\frac{k_2\Delta\delta_{long} + (\mathbf{k}_3 - \zeta\mathbf{k}_4)\begin{bmatrix} \Delta q \\ \Delta B_1 \end{bmatrix}}{(\zeta k_2 - k_1)\Delta\delta_{long} + (\zeta\mathbf{k}_3 + \beta^2\mathbf{k}_4)\begin{bmatrix} \Delta q \\ \Delta B_1 \end{bmatrix}}\right) \tag{14}$$

Substituting the time to peak of eqn. 14 into the time response in eqn. 13 gives the peak response of the longitudinal flapping. The resulting equation returns peak flapping response for a longitudinal stick input, given the following data:

- Current values of pitch rate and longitudinal cyclic, provided by onboard sensors.
- Local linear dynamics matrices and equilibrium parameters., scheduled with flight condition.
- Current instantaneous flapping angle, given by the neural network.

The next step is to derive the magnitude of the control deflection that will cause the flapping response to impinge upon the mechanical limits. This results in a constraint on the longitudinal stick that will ensure that the flapping limit is not exceeded. Since the peak response is a complex non-linear function of the control deflection, an iterative process is needed to solve for the control stick constraints.

$$\beta_{\lim} = f\left(\delta_{long\,\lim}, \beta_{long}, q, B_1, \mathbf{A}, \mathbf{B}, \mathbf{C}, \mathbf{x}_e\right) \quad \text{solve for } \delta_{\mathrm{long}_{\lim}} \qquad \textbf{(15)}$$

Fortunately, a simple fixed-point iteration proves to be adequate in solving the non-linear system to within reasonable accuracy after 10-20 iterations.

The algorithm is applied to limit the peak response of a limited parameter as shown in the schematic in Figure 12. The system was applied to limit longitudinal flapping on the XV-15 and evaluated in batch simulation. The flapping limits were set to 10° aft and 8° forward.

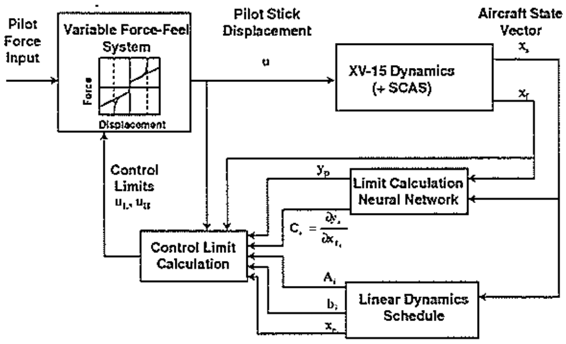

Figure 12 Peak Response Limiting System

A series of large amplitude doublet inputs on the longitudinal cyclic stick were simulated. A full amplitude doublet input is commanded, but the actual inputs are restricted within the constraints calculated by the limiting system. In an actual system these constraints would be relayed to the pilot with dynamic soft stop cues. Figure 13 shows the flapping response and stick position for a set of doublet inputs that accelerate the aircraft from 20 to 50 knots. The dashed line in the stick position plot shows the control constraints calculated by the flapping limiting algorithm. The flapping response shows that the longitudinal flapping approaches but does not exceed the prescribed limits. The results show that the control stick limits vary with time. There is an initial position constraint on the stick position, and then the constraint is relaxed resulting in an effective rate limit on the stick movement, during which the flapping angle is held right at the prescribed limit. The most severe restrictions on stick travel occur for the stick reversal. The airspeed changes throughout the maneuver, but the scheduling of the linear models provides adequate modeling of the flapping dynamics.

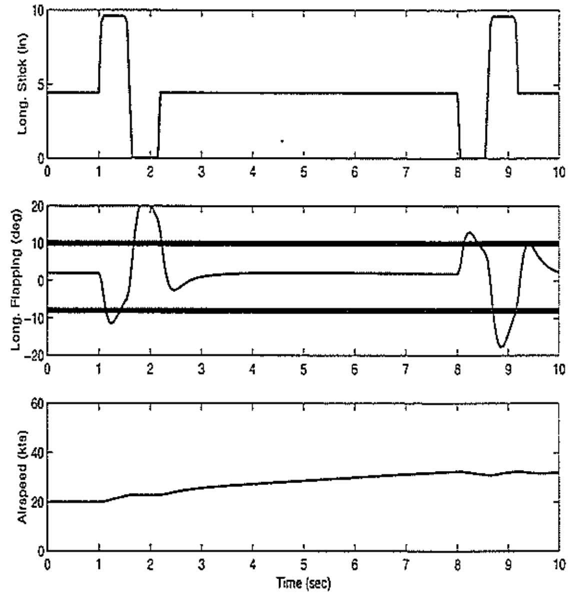

Figure 13 Doublet Input with No Limit Avoidance

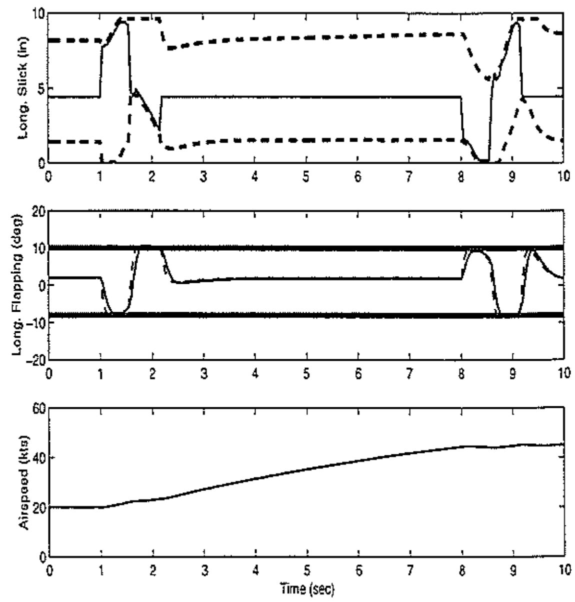

Figure 14 Doublet Input with Limit Avoidance

The system was also evaluated for a full magnitude frequency sweep at 40 knots. The commanded input is a sinusoid with varying frequency. Figure 15 shows the resulting control input and flapping response. The results show that the flapping angle is constrained within the envelope limits. As expected, the maximum allowable control deflections become more restricted at higher frequencies, around the short period mode.

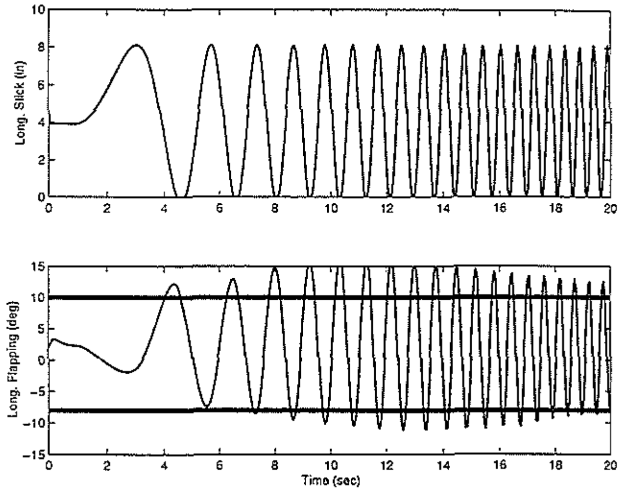

Figure 15 Frequency Sweep with No Limit Avoidance

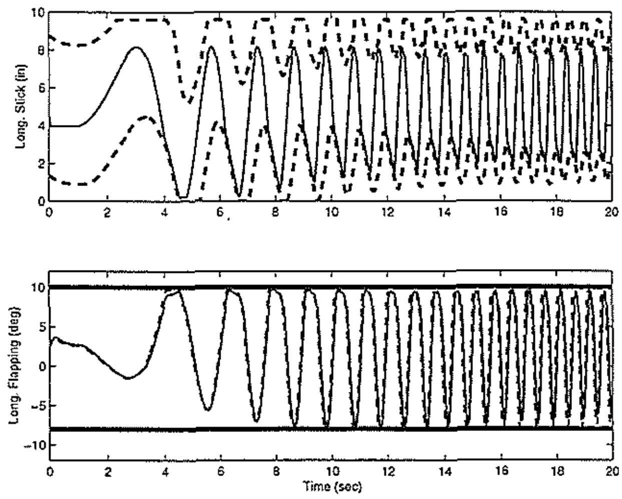

Figure 16 Frequency Sweep with Limit Avoidance

Figure 17 shows the frequency response of longitudinal flapping to a maximum amplitude sinusoidal cyclic stick input at 40 knots. The figure shows the flapping frequency response for:

- The non-linear simulation without limiting.
- The simplified 2nd order linear model used by the limiting algorithm.
- The full, 10th order linear model, from which the simplified model is derived.
- The response with envelope limiting engaged.

The graph shows that the simplified linear model is a good approximation of the full linear dynamics in the most critical frequency range, 1 to 20 rad/sec. As expected, the simplified model ignores the phugoid mode, but this mode occurs at very slow frequencies where a prediction lead time is not important. It is not critical to have an accurate linear model over very low frequencies. The results also show that the linear models are a reasonably good approximation of the non-linear simulation in the critical frequency range. Discrepancies can be attributed to non-linearities, and the fact that airspeed varied significantly during the non-linear simulations (±20 knots).

The linear and non-linear simulation results without limiting are based on 4.2 inch stick deflections from trim. When the flapping protection is engaged the available control travel is reduced, and the results show that system effectively limits the flapping response to within the envelope limits, which are ±9° from trim in the 40 kts flight condition.

5. Conclusions

Three different approaches to envelope protection were developed. Dynamic trim estimation has been shown to be an effective tool for cueing pilots of approaching envelope limits that are reached in steady-state flight. The system was demonstrated in piloted simulations of the V-22. The system has the advantage that direct sensor measurement of the limit is not necessary, but has the possible disadvantage that a large quantity of training data is required to account for all possible weight and balance configurations. If direct measurement of the envelope limit is available, then adaptive dynamic trim estimation is an effective alternative. By supplementing the dynamic trim estimation algorithm with an adaptive neural network, the system showed the capability to adapt to large variations in weight and balance parameters.

Some limited parameters such as rotor flapping tend to impinge upon limits in the peak transient response. A technique was developed to predict peak response characteristics based on simplified linear models of the limit dynamics about the dynamic trim equilibria. The capability of the system to protect against longitudinal flapping limits was investigated using batch simulations of the XV-15. The system proved to be quite successful in determining constraints on the longitudinal control stick which ensure that the longitudinal flapping limits are not exceeded. Equivalent results were shown in both time and frequency domain.

6. Acknowledgements

This work was funded under the NRTC Center of Excellence in Rotorcraft Technology at the Georgia Institute of Technology, contract No. NRC 2-945. Real-time simulations were carried out at the Boeing Helicopters Flight Simulation Laboratory in Philadelphia, PA.

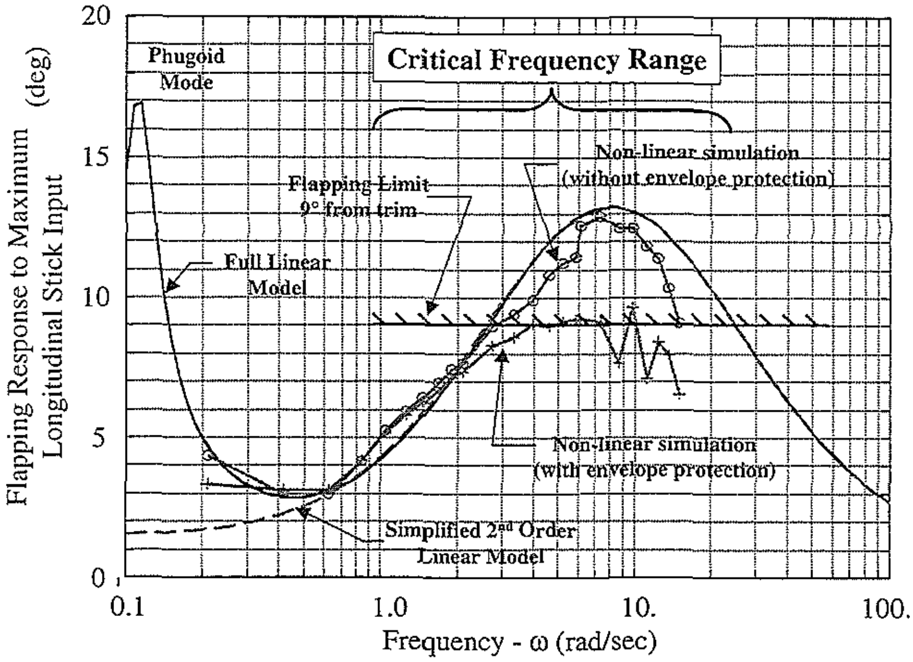

Figure 17 Flapping Response of Linear Models and Non-Linear Simulation

7. References

1. Corps, S.G., "Airbus A320 Side Stick and Fly By Wire - An Update", Proceedings of SAE 5th Aerospace Behavioral Engineering Technology Conference, Long Beach, CA, 1987.
2. Iloputaife, O., "Design of Deep Stall Protection for the C-17A", AIAA Guidance, Navigation, and Control Conference, San Diego, CA, July, 1996.
3. Howitt, J., "Carefree Handling for Super-Agility", American Helicopter Society Aeromechanics Specialist Conference, Fairfield County, Connecticut, October 1995.
4. Howitt, J., "Carefree Maneuvering in Helicopter Flight Control", American Helicopter Society 51st Annual Forum, Fort Worth, TX, May 1995.
5. Kimball, D.F., "Recent Tilt Rotor Flight Control Law Innovations", *AHS Journal*, 1987.
6. Miller, D.G. and Black, T.M., "Tiltrotor Control Law Design for Rotor Loads Alleviation Using Modern Control Techniques", American Control Conference, June 1991.
7. King, D.W., et. al., "V-22 Load Limiting Control Law Development", American Helicopter Society 49th Annual Forum, St. Louis, Missouri, May, 1993.
8. Whalley, M.S. and Achache, M., "Joint U.S./France Investigation of Helicopter Flight Envelope Limit Cueing", American Helicopter Society 52nd Annual Forum, Washington, D.C., June, 1996.
9. Whalley, M.S., A Piloted Simulation Investigation of a Helicopter Limit Avoidance System Using a Polynomial Neural Network, NASA/TM-1998-112220, January, 1998.
10. Haas, D.J., Flitter, L.A., and Milano, J., "Helicopter Flight Data Feature Extraction or Component Load Monitoring", AIAA 35th Structures, Structural Dynamics, and Materials Conference, Hilton Head, SC, April, 1994.
11. Haas, D.J., McCool, K., and Flitter, L.A., "Development and Flight Test Evaluation of a Rotor System Load Monitoring Technology", American Helicopter Society 54th Annual Forum, Washington, D.C., May, 1998.
12. Horn, J., Calise, A.C., Prasad, J.V.R, and O'Rourke, M., "Flight Envelope Cueing on a Tilt-Rotor Aircraft Using Neural Network Limit Prediction", American Helicopter Society 54th Annual Forum, Washington, D.C., May, 1998.
13. Horn, J., Calise, A.C., and Prasad, J.V.R, "Flight Envelope Limiting Systems Using Neural Networks", AIAA Atmospheric Flight Mechanics Conference, Boston, MA, August, 1998.
14. Horn, J., Calise, A.C., and Prasad, J.V.R, "Development of Envelope Protection Systems for Rotorcraft", American Helicopter Society 55th Annual Forum, Montreal, Canada, May, 1999.
15. NASA CR-166536, A Mathematical Model for Real Time Flight Simulation of a Generic Tilt-Rotor Aircraft, Sept. 1988, Rev. A.
16. Rysdyk, R.T. and Calise, A.J., "Adaptive Model Inversion Flight Control for Tilt-Rotor Aircraft", American Helicopter Society 54th Annual Forum, Washington, D.C., May, 1998.